Electronic Supplementary Information

Facile fabrication of fluorescent Fe-doped carbon quantum dots for dopamine sensing and bioimaging application

Shujuan Zhuo,*[ab] Yuanyuan Guan,[a] Hui Li,[a] Jing Fang,[a] Ping Zhang,[a] Jinyan Du[a] and Changqing Zhu*[a]

[a]Key Laboratory of Functional Molecular Solids, Ministry of Education; Anhui Key Laboratory of Chemo-Biosensing, College of Chemistry and Materials Science, Anhui Normal University, Wuhu, 241000, PR China
[b]Anhui Meijia New Materials Company Limited, Wuhu, 241000, PR China

*Corresponding authors, E-mail addresses: sjzhuo@mail.ahnu.edu.cn (S. Zhuo), zhucq@mail.ahnu.edu.cn (C. Zhu).

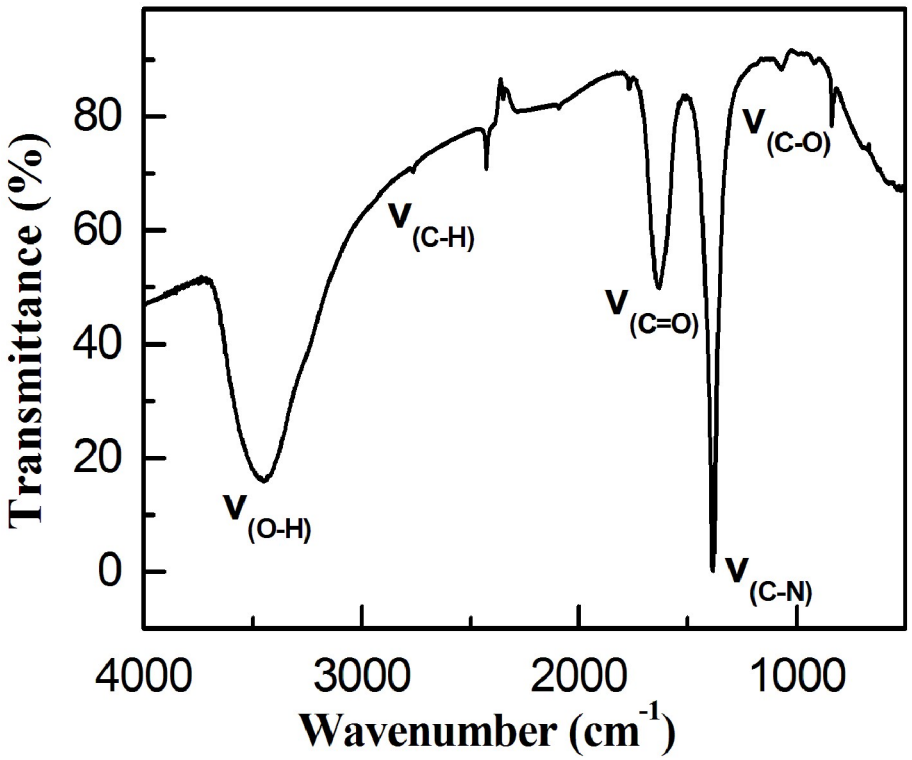

Fig. S1 FT-IR spectrum of the as-prepared Fe-CQDs.

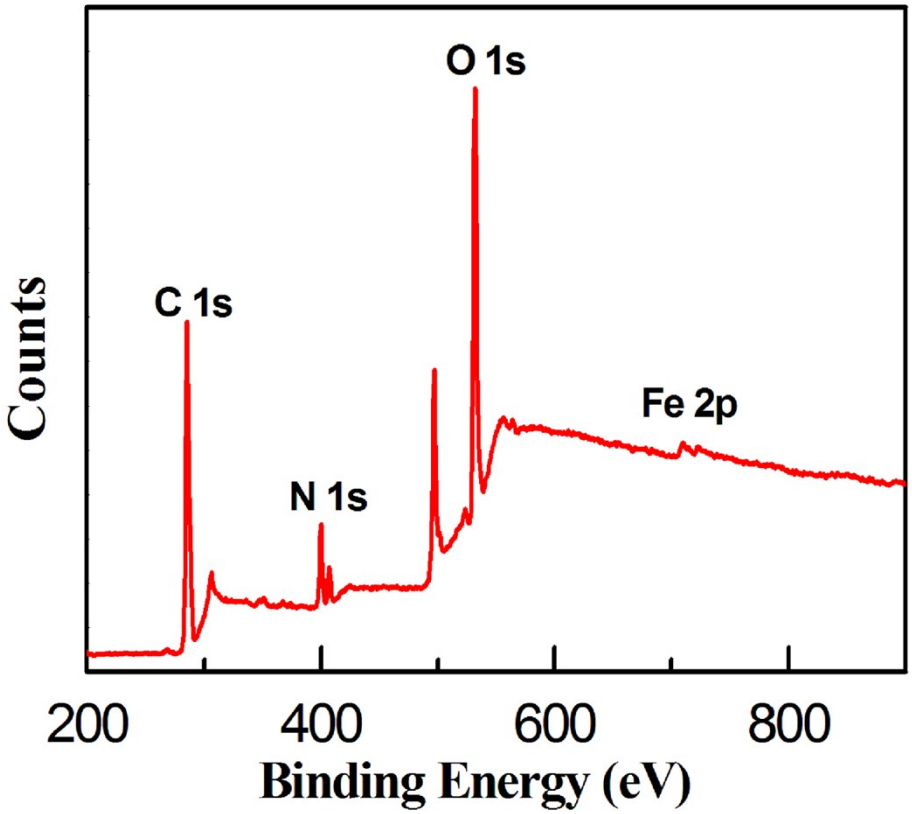

Fig. S2 Wide scan XPS full spectrum of Fe-CQDs.

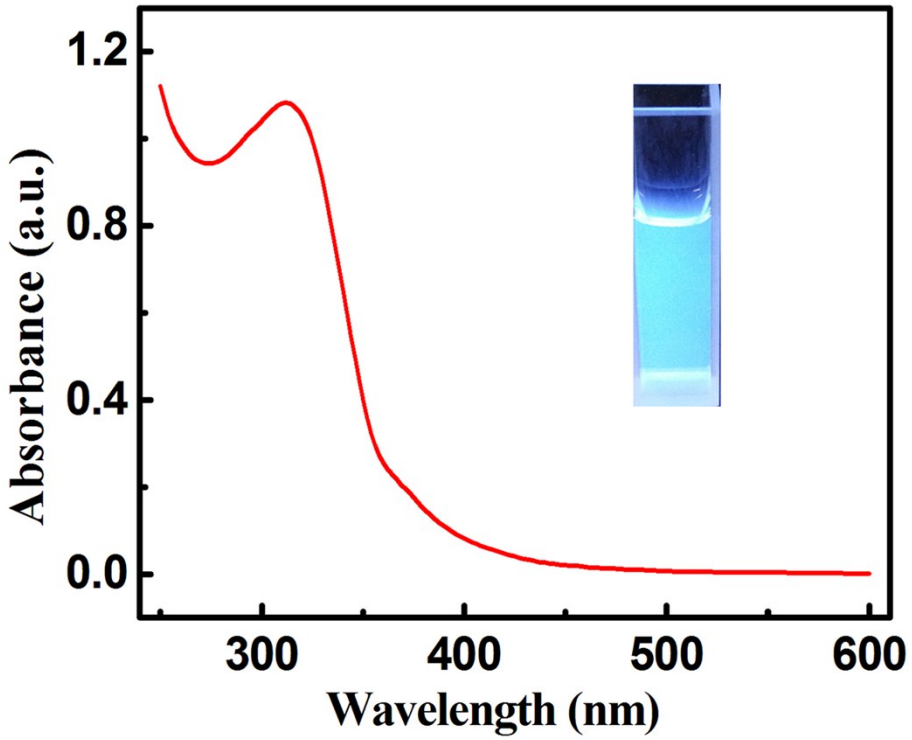

Fig. S3 UV-vis absorption spectrum of the Fe-CQDs. Insert: the optical photograph of the Fe-CQDs dispersed in water illuminated under UV light (365 nm).

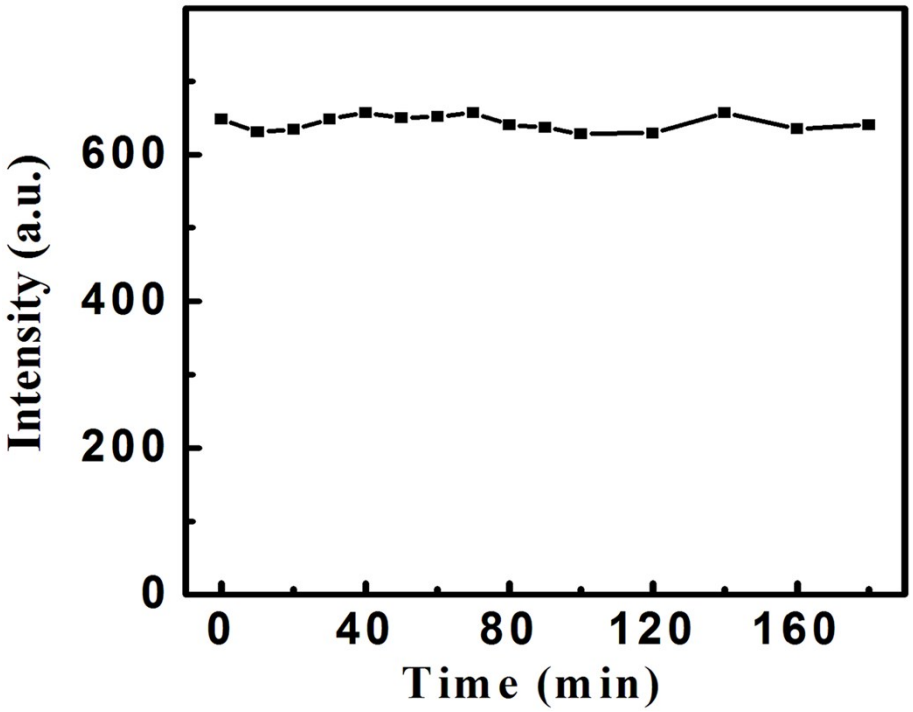

Fig. S4 The stability of Fe-CQDs over time under the UV light irradiation.

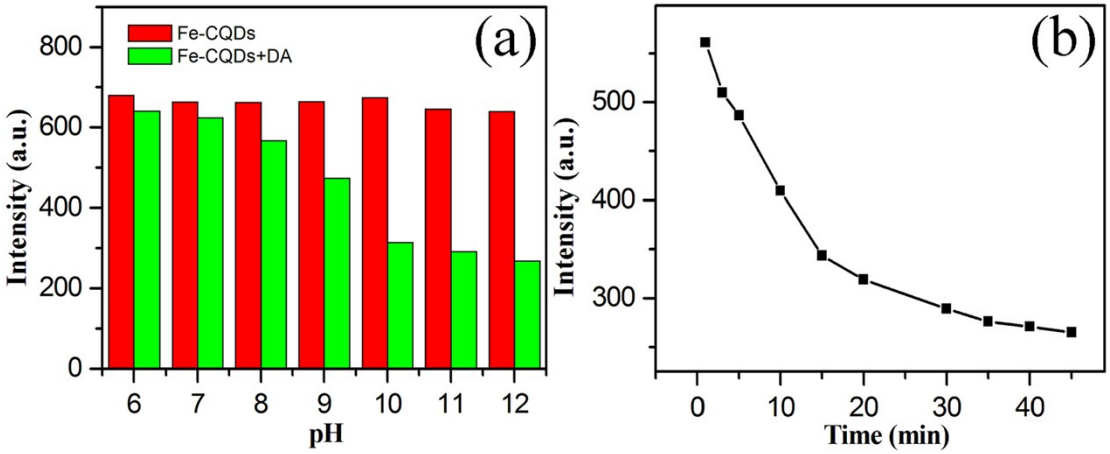

Fig. S5 (a) Effect of pH on the detection of dopamine. (b) Effect of incubation time on the fluorescence intensity of the Fe-CQDs-DA system. The concentration of DA is 50 μM.

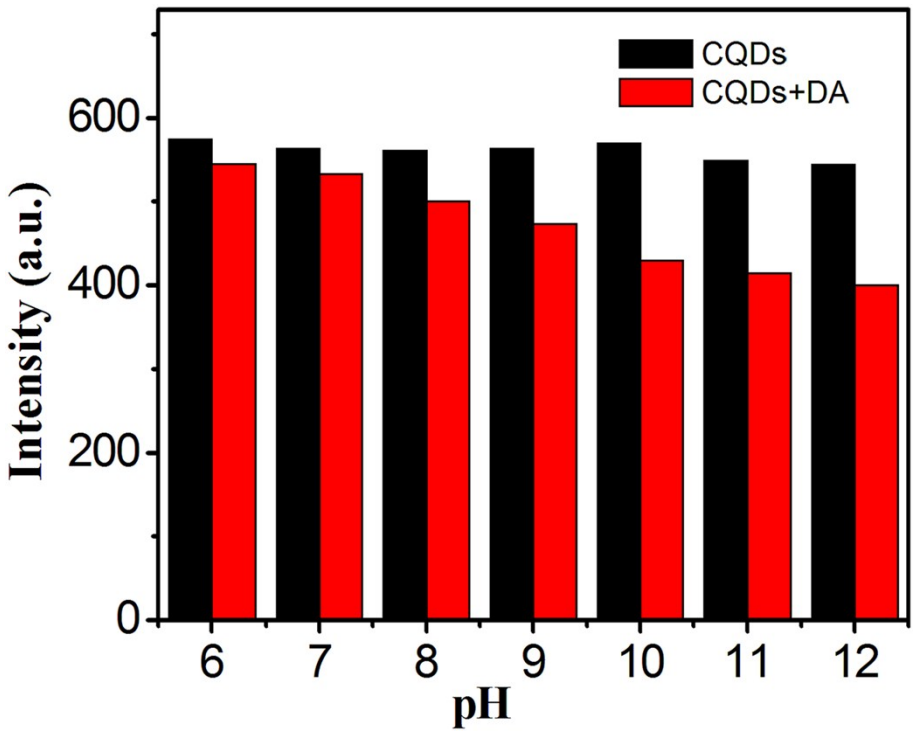

Fig. S6 Effect of pH on fluorescence intensity of the CQDs-DA system.

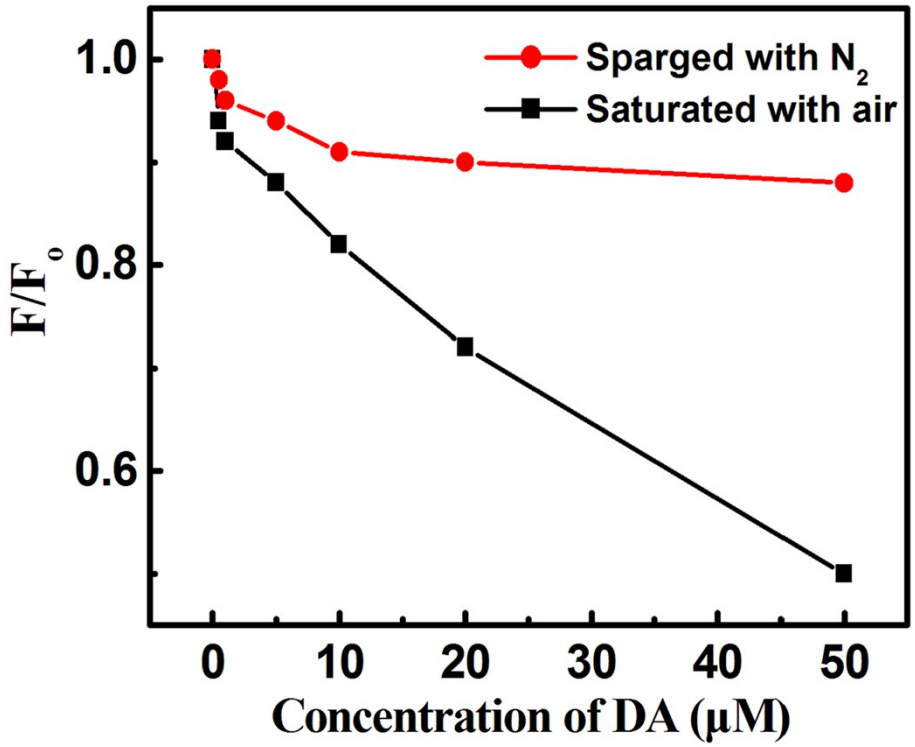

Fig. S7 Comparison of quenching efficiency between nitrogen-saturated (red line) and oxygen-saturated system (black line). F_0 and F are fluorescent intensities of the Fe-CQDs without and with dopamine, respectively.

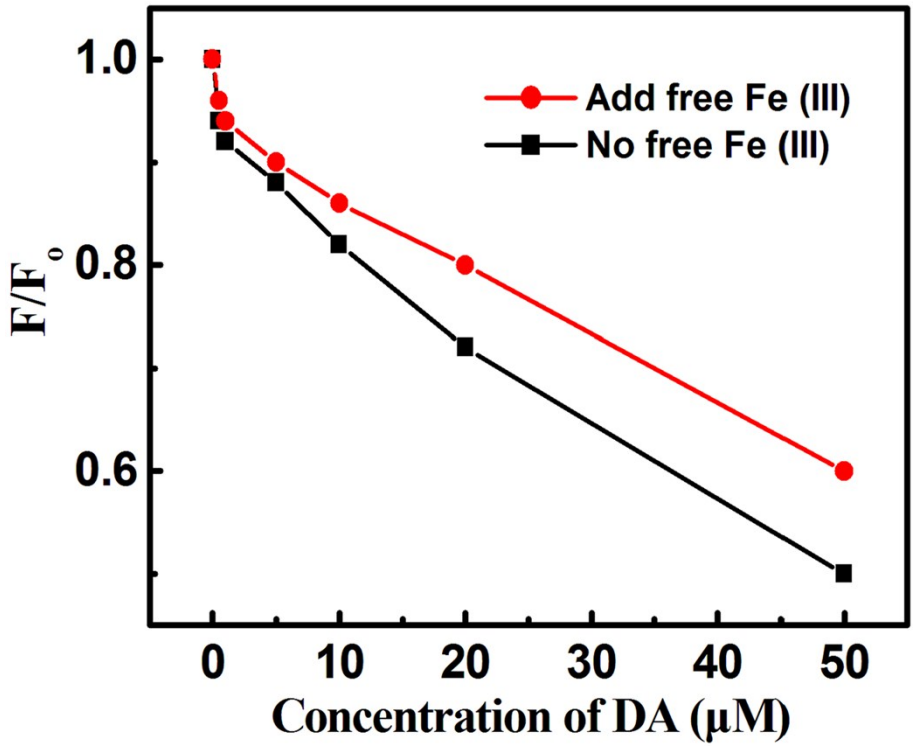

Fig. S8 Comparison of quenching efficiency in the presence (red line) and absence of free iron(III) ion (black line).

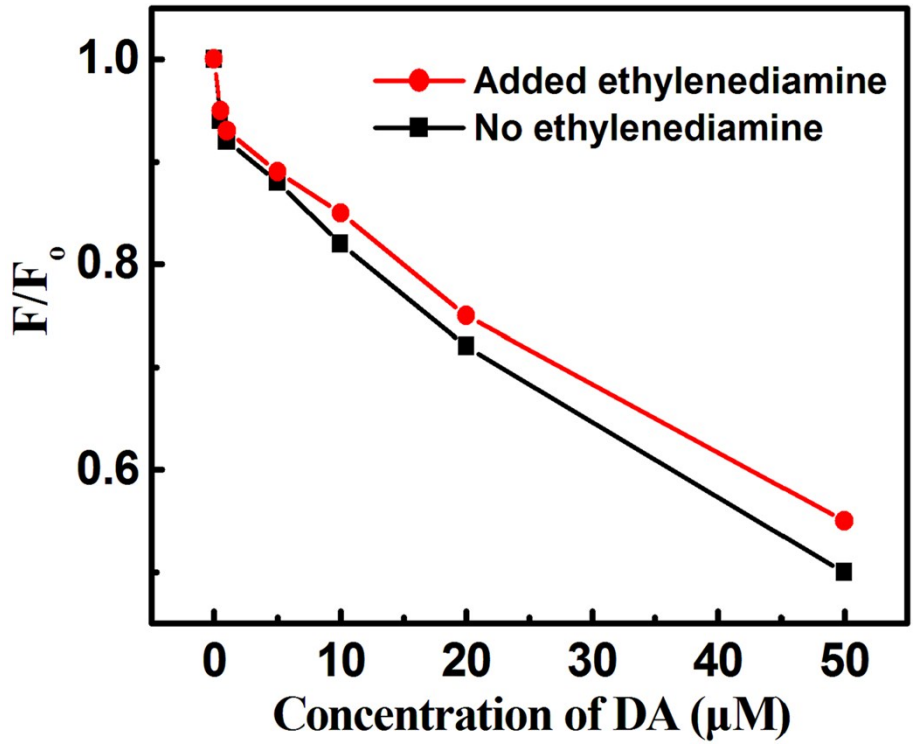

Fig. S9 Comparison of quenching efficiency in the presence (red line) and absence of ethylenediamine (black line).

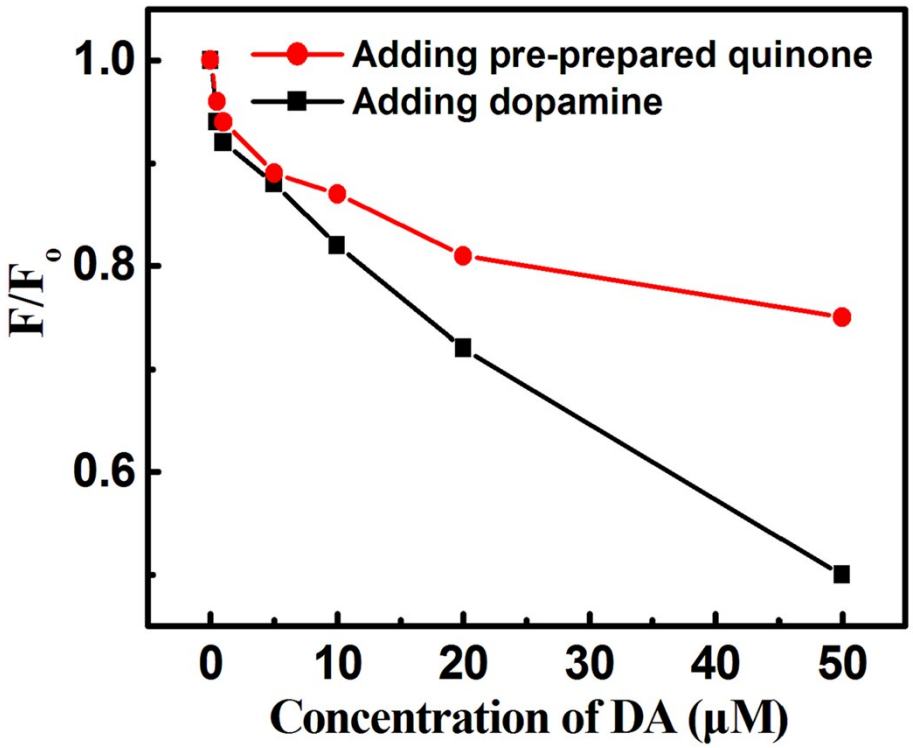

Fig. S10 Comparison of quenching efficiency by adding pre-prepared quinone (red line) and dopamine (black line).

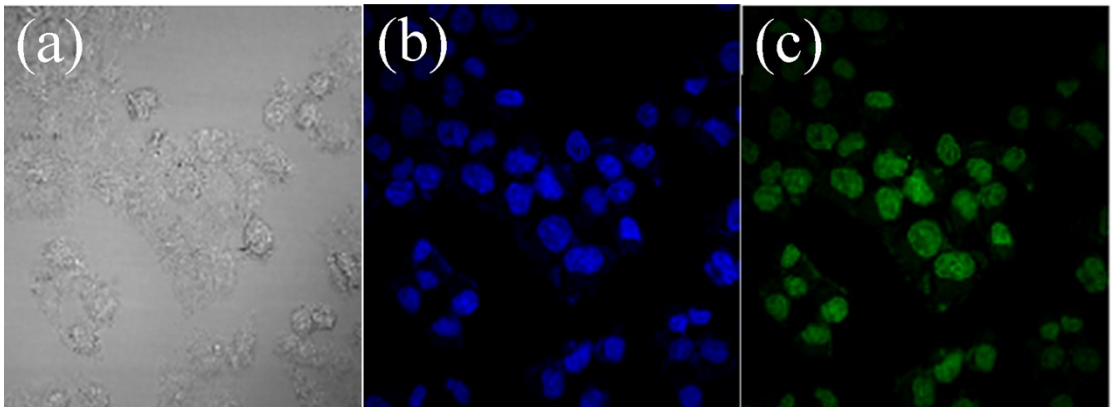

Fig. S11 Confocal fluorescence images of HeLa cells labeled with Fe-CQDs. (a) HeLa cells under bright field, by excitation at (b) 405 nm and (c) 488 nm.

Table S1 A brief summary of different nanomaterials-based fluorescence probes for the detection of DA.

Probe system	Linear range (μM)	Detection limit (nM)	Refs.
Abtz-CdI_2-MOF	0.25-50	57	1
MoS_2 nanohybrid	0.0025-5	0.9	2
Carbon dots	0.1-3	37	3
β-CD@AuNCs	0.1-80	20	4
BSA-CuNCs	0.5-50	280	5
pDA NPs	0.01-5	5.5	6
Resorcinol	0.01-20	1.8	7
CDs/CuNCs nanohybrid	0.1-100	32	8
CDots-AuNCs hybrid	0.005-0.18	2.9	9
r-QDs@SiO_2-PDA	10-80	120	10
Fe-CQDs	0.01-50	5	This work

References

1 Y. Cheng, J. Wu, C. Guo, X. G. Li, B. Ding and Y. Li, *J. Mater. Chem. B,* 2017, **5**, 2524–2535.

2 N. P. Mani, M. Ganiga and J. Cyriac, *Analyst,* 2018, **143**, 1691–1698.

3 F. Qu, W. Huang and J. M. You, *Colloid. Surface B,* 2018, **162**, 212–219.

4 M. I. Halawa, F. X. Wu, T. H. Fereja, B. H. Lou and G. B. Xu, *Sens. Actuator. B,* 2018, **254**, 1017–1024.

5 Z. Miao, W. L. Hou, M. L. Liu, Y. Y. Zhang and S. Z. Yao, *New J. Chem.,* 2018, **42**, 1446–1456.

6 Y. J. Pang, Y. Shi, Y. D. Pan, Y. F. Yang, Y. J. Long and H. Z. Zheng, *Sens. Actuator. B,* 2018, **263**, 177–182.

7 X. L. Zhang, Y. G. Zhu, X. Li, X. H. Guo, B. Zhang, X. Jia and B. Dai, *Anal. Chim. Acta,* 2016, **944**, 51–56.

8 W. J. He, R. J. Gui, H. Jin, B. Q. Wang, X. N. Bu and Y. X. Fu, *Talanta,* 2018, **178**, 109–115.

9 Y. S. He, C. G. Pan, H. X. Cao, M. Z. Yue, L. Wang and G. X. Liang, *Sens. Actuator. B,* 2018, **265**, 371–377.

10 M. Yu, Y. Lu and Z. Tan, *Talanta,* 2017, **168**, 16–22.